Cavity QED with atomic mirrors

New Journal of Physics

Cavity QED with atomic mirrors

D E Chang[1,4]**, L Jiang**[2]**, A V Gorshkov**[2] **and H J Kimble**[2,3]

[1] ICFO—Institut de Ciencies Fotoniques, Mediterranean Technology Park, 08860 Castelldefels, Barcelona, Spain
[2] Institute for Quantum Information and Matter, California Institute of Technology, Pasadena, CA 91125, USA
[3] Norman Bridge Laboratory of Physics 12-33, California Institute of Technology, Pasadena, CA 91125, USA
E-mail: darrick.chang@icfo.es

Abstract. A promising approach to merge atomic systems with scalable photonics has emerged recently, which consists of trapping cold atoms near tapered nanofibers. Here, we describe a novel technique to achieve strong, coherent coupling between a single atom and photon in such a system. Our approach makes use of collective enhancement effects, which allow a lattice of atoms to form a high-finesse cavity within the fiber. We show that a specially designated 'impurity' atom within the cavity can experience strongly enhanced interactions with single photons in the fiber. Under realistic conditions, a 'strong coupling' regime can be reached, wherein it becomes feasible to observe vacuum Rabi oscillations between the excited impurity atom and a single cavity quantum. This technique can form the basis for a scalable quantum information network using atom–nanofiber systems.

---

[4] Author to whom any correspondence should be addressed.

IOP Institute of Physics Φ DEUTSCHE PHYSIKALISCHE GESELLSCHAFT

Contents

Techniques to controllably interface atoms with quantum optical fields form the basis for many applications in quantum information science [1, 2]. For example, photons are convenient to relay information over large quantum networks, while atoms are naturally physical systems that can process and store this information. Thus far, the available techniques to efficiently couple single photons with atomic media fall into one of the following, mostly independent, categories: (i) cavity quantum electrodynamics (QED) [3–5], where atomic interactions with light are enhanced via a high-finesse cavity; (ii) coherent coupling with atomic ensembles exhibiting large optical depths [6]; and (iii) the use of fields tightly focused to dimensions smaller than or approaching the scattering cross-section of a single atom [7–12]. Although remarkable achievements have been made with all of these approaches, a robust, scalable technique that can be easily integrated with photonics remains elusive.

Here, we describe a hybrid strategy that combines appealing attributes of each of the methods described above, and which can be implemented with relatively modest resources. Our approach utilizes a promising atom–light interface developed in recent years, which consists of cold atoms trapped near tapered nanofibers [13–15]. The traps are well characterized [13, 14, 16] and can potentially be used to transport and couple atoms to other systems, such as dielectric optical cavities [17, 18] and nanomechanical resonators [19, 20]. The nearly diffraction-limited transverse confinement of optical fields thus far enables $\sim$1–10% coupling efficiency of a single atom to the fiber [13–15], which has allowed for observations of strong light–matter interactions using relatively few atoms and low powers [21–23].

Our hybrid approach is based upon the following principles. First, we show that although the single-atom coupling in this system might be relatively weak, there exist collective modes of a trapped atomic ensemble whose coupling to light is enhanced by the square root of the atom number, $\sqrt{N_A}$ [6]. While collective effects are generally well known, special consequences emerge in the nanofiber system when the atoms are trapped in a lattice. In particular, collective effects cause such a lattice to act as a near-perfect mirror for an incident field close to resonance. In analogy to cavity QED, we then demonstrate that two sets of atomic mirrors can form an effective cavity, which can greatly enhance the coupling of a *single*, specially chosen 'impurity' atom (or a few impurity atoms) positioned inside. We introduce a novel quantum spin model to describe the atom–light coupling, which allows one to exactly map the atom–nanofiber interface onto the simple and elegant Jaynes–Cummings model of cavity QED [24]. A unique feature of our atomic mirrors compared to conventional cavities is that they have long relaxation times and are highly dispersive. Remarkably, even with very low mirror finesse ($F \sim 10^2$) this property allows one to attain the 'strong coupling' regime of cavity QED [3–5], where vacuum Rabi oscillations [3, 25–27] occur between an excited impurity atom and a single

'photon' stored in the cavity (or more precisely, in the atomic mirrors). Furthermore, as quantum mechanical objects, these atom mirrors can be used to store quantum information and transfer this information into propagating waveguide modes. We describe how these various features can be combined to realize all of the building blocks for scalable quantum information processing.

1. Atom–nanofiber interface: linear spectral properties

We model our system as an ensemble of two-level atoms with ground and excited states $|g\rangle$, $|e\rangle$ and resonance frequency ω_A, located at positions z_j. These atoms interact with a one-dimensional (1D) waveguide supporting left- and right-propagating fields $\hat{E}_{L,R}$ with linear dispersion and velocity v through a dipolar coupling, $H_{int} = -\hbar\beta\sqrt{2\pi}\sum_j[\sigma_{eg}^j(\hat{E}_R(z_j) + \hat{E}_L(z_j)) + \text{h.c.}]$. This coupling yields the Maxwell–Bloch equations for the field propagation [28] with solutions
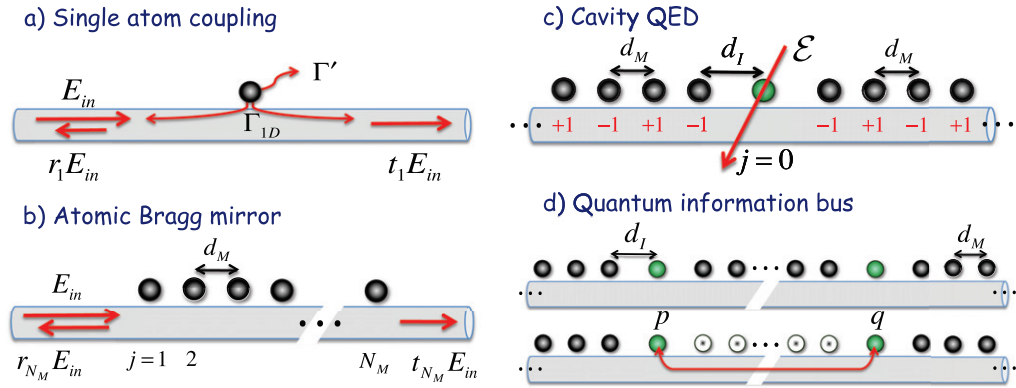
$$\hat{E}_{R(L)}(z, t) = \hat{E}_{R(L),in}(z \mp vt) + \frac{\sqrt{2\pi}i\beta}{v}\sum_j \Theta\left(\pm(z - z_j)\right)\sigma_{ge}^j(t \mp (z - z_j)/v), \tag{1}$$

where $\Theta(z)$ is the Heaviside step function and $\hat{E}_{R(L)}(z \mp vt)$ are the homogenous solutions corresponding to the right- and left-propagating incident fields. The single-atom spontaneous emission rate into the waveguide is $\Gamma_{1D} = 4\pi\beta^2/v$ [28]. In addition to equation (1), H_{int} yields the usual Heisenberg equations for the atomic coherence operators $\sigma_{ge}^j = |g_j\rangle\langle e_j|$. We also assume that each atom independently emits into free space with rate Γ', such that the total emission rate of a single atom is $\Gamma = \Gamma' + \Gamma_{1D}$ (see figure 1(a)).

The transfer matrix formalism of [29] is well suited to solve for linear or single-photon propagation through the ensemble. From equation (1), one first finds the single-atom reflection and transmission amplitudes of an incident field [28], as shown in figure 1(a). We find that $r_1(\Delta_A) = -\Gamma_{1D}/(\Gamma - 2i\Delta_A)$ and $t_1(\Delta_A) = 1 + r_1(\Delta_A)$, where $\Delta_A = \omega_P - \omega_A$ is the detuning between the field input frequency ω_P and the atomic resonance. In addition, free-space propagation over a distance d is characterized by multiplicative phase shifts, $E_{R(L)}(z + d) = e^{\pm i\omega_P d/v}E_{R(L)}(z)$. The field scattering from many atoms can then be exactly summed using transfer matrices [29], from which the total system reflection and transmission amplitudes are obtained.

We now focus on the case where N_M atoms are arranged periodically with a lattice constant of $d_M = \pi v/\omega_A \equiv \lambda_A/2$ to form an atomic 'Bragg mirror', as shown in figure 1(b) (analogous results hold when d_M is any other integer multiple of half the resonant wavelength λ_A). For atom number $N_M \lesssim N_{gap} \equiv \sqrt{\omega_A/\Gamma_{1D}}$, the effect of small detunings from resonance is negligible in free propagation, and one can approximate $e^{\pm i\omega_P d_M/v} \approx -1$. The reflectance from the lattice in this regime is given by a broadened Lorentzian, $R_{N_M}(\Delta_A) = \frac{(N_M\Gamma_{1D})^2}{(\Gamma'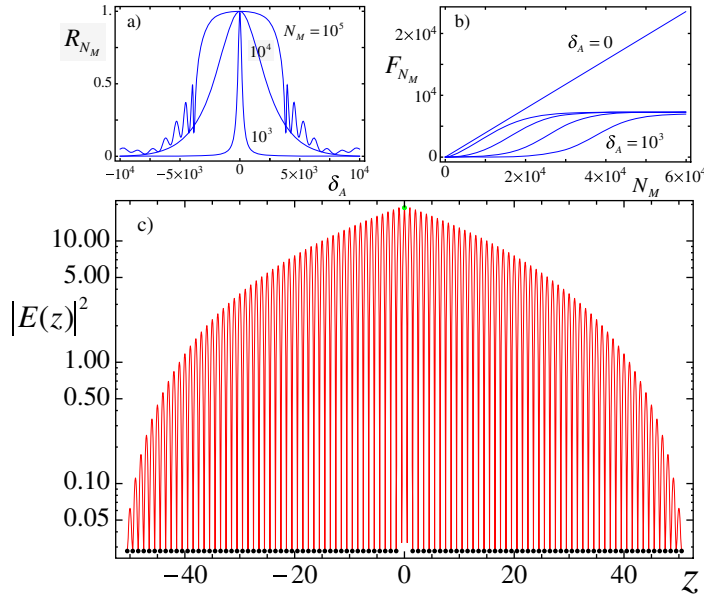 + N_M\Gamma_{1D})^2 + 4\Delta_A^2}$ (see figure 2(a)), while the transmittance is $T_{N_M}(\Delta_A) = \frac{\Gamma'^2 + 4\Delta_A^2}{(\Gamma' + N_M\Gamma_{1D})^2 + 4\Delta_A^2}$. For $N_M \gtrsim N_{gap}$, the resonant reflectance approaches unity with increasing atom number, $R_{N_M}(\Delta_A = 0) = (\frac{N_M\Gamma_{1D}}{\Gamma' + N_M\Gamma_{1D}})^2$, but the phases accumulated in free propagation for finite detuning cannot be neglected. Away from resonance, the lattice forms a band gap for detunings $|\Delta_A| < \sqrt{\omega_A\Gamma_{1D}}/\pi$, over which the reflectance saturates as $N_M \to \infty$ to a value $1 - R_{N_M} \sim \mathcal{O}(\sqrt{\Gamma'^2/(\omega_A\Gamma_{1D})})$. The deviation from perfect reflection occurs because of atomic scattering of light into free space, in contrast to the perfect gap formed by purely dispersive media. Similar results have been derived for the present

Figure 1. Different configurations of a coupled atom–fiber system. (a) Single-atom coupling. The atom spontaneously emits into the fiber and free space at rates Γ_{1D} and Γ', respectively. In the linear regime, the atom scatters a guided input field E_{in} with reflection and transmission amplitudes r_1, t_1. (b) N_M atoms in a chain with lattice constant d_M form an atomic 'Bragg mirror', with linear reflection and transmission amplitudes r_{N_M}, t_{N_M}. (c) In the 'cavity QED' configuration, two atomic Bragg mirrors (located at $1 \leqslant j \leqslant N_M$ and $-N_M \leqslant j \leqslant -1$) form a cavity, which enhances the coupling of an impurity atom (green, $j = 0$) to the fiber. The distance between the impurity and its nearest neighbors is d_I. The relative phases ± 1 of the mirror atom spin wave comprising the cavity excitation are denoted in red. An external field $\mathcal{E}$ can be used to drive the impurity atom. (d) Quantum information transfer can occur between two well-separated impurity atoms p, q in the 'quantum information bus' configuration. Here the two impurity atoms initially sit in separate cavities within a long chain of mirror atoms (dark circles). Then, all the mirror atoms between them are flipped into a transparent hyperfine state $|s\rangle$ (white). This process loads the impurity atoms into a new, common cavity mode defined by the remaining mirror atoms positioned external to p, q.

geometry [30] and for atoms trapped in a 1D standing wave in free space [29], as well as observed in the latter case [31, 32]. Band structures in other atomic configurations have also been explored [33, 34]. In the following, we will primarily consider the regime $N_M \lesssim N_{gap}$, which is more readily attainable for current experiments.

A remarkable consequence of the system periodicity is that a lattice of many atoms can form a nearly perfect mirror around resonance with $1 - R_{N_M} \approx 2\Gamma'/(N_M\Gamma_{1D})$, even if a single atom is mostly absorptive ($\Gamma' > \Gamma_{1D}$). As shown below, this effect arises from the excitation of a collective super-radiant atomic mode whose coupling with the waveguide is strongly enhanced. This expression reproduces the known result [28, 35] that a single emitter ($N_M = 1$) can have strong reflectance when $\Gamma_{1D}/\Gamma' \gg 1$, which can physically occur when atoms are coupled to extremely narrow metallic nanowires [10]. Our result is appealing as it demonstrates that using extremely small guiding structures can be avoided simply by having optical depth as a resource. The collective interaction in our system produces a number of other interesting phenomena as well. Firstly, the envelope of a propagating field attenuates through the lattice in a non-exponential manner, as plotted in figure 2(c) across sites $1 < j < N_M$. However, each atom sees

Figure 2. Atom mirror properties. (a) Reflectance $R_{N_M} = |r_{N_M}(\delta_A)|^2$ of a mirror comprised of an atomic chain, as a function of dimensionless detuning $\delta_A = \Delta_A/(\Gamma/2)$. The spectra are shown for mirror atom numbers $N_M = 10^3, 10^4, 10^5$. The reflectance becomes non-Lorentzian for atom numbers $N_M \gtrsim N_{gap} \equiv \sqrt{\omega_A/\Gamma_{1D}} \approx 1.6 \times 10^4$. (b) Effective cavity finesse, defined as $F_{N_M} \equiv \pi/(1 - R_{N_M}(\delta_A))$, of an atomic chain as a function of mirror atom number N_M. The finesse is shown for detunings $\delta_A = 0, 30, 100, 300, 1000$. (c) Two atom mirrors surrounding an impurity atom form an effective cavity, as illustrated in figure 1(c). The intra-cavity intensity $|E(z)|^2 = |E_R(z) + E_L(z)|^2$ is plotted as a function of position (in units of the atomic site number j), when the impurity atom is externally driven on resonance. $|E(z)|^2$ is normalized by the intensity produced by a single atom driven on resonance under the same external amplitude $\mathcal{E}$, in the absence of mirror atoms. The black and green points depict the local fields at the mirror and impurity atom sites, respectively. We have used parameters $\Gamma_{1D} = \Gamma'/4$ and $\omega_A/\Gamma = 5.4 \times 10^7$ for all panels in this figure.

the *same*, site-independent local field intensity, given on resonance by $|E(z_j)/E_0|^2 = \frac{\Gamma'^2}{(\Gamma' + N_M\Gamma_{1D})^2}$, where E_0 is the peak amplitude. The fact that each atom sits progressively closer to the nodes with increasing N_M suppresses free-space scattering and builds up the large reflection amplitude. Although the lattice is highly reflective on resonance, it is also 'dark', in that the remaining light is mostly scattered by the atoms into free space as opposed to transmitted, $\mathcal{L}_{N_M} \equiv 1 - R_{N_M} - T_{N_M} \gg T_{N_M}$. The mirror can be made mostly dispersive ($\mathcal{L}_{N_M} \ll T_{N_M} \ll R_{N_M}$) by operating in a range of detunings where $N_M\Gamma_{1D} \gg |\Delta_A| \gg \sqrt{N_M\Gamma_{1D}\Gamma'}$, at the expense of needing more atoms to reach a given reflectance.

These collective modes can be leveraged to produce strong coupling between the fiber and a *single*, specially chosen atom from within the ensemble. This approach is illustrated in the 'cavity QED' configuration of figure 1(c). As the nomenclature suggests, here two atomic Bragg mirrors (at positions $-N_M \leq j \leq -1$ and $1 \leq j \leq N_M$, for $N_A = 2N_M$ total mirror atoms)

form an effective cavity for an impurity atom located between them at $j = 0$. The impurity atom is located a distance d_I from its nearest neighbors. We will focus on the geometry where $d_I = 3\lambda_A/4$ and $d_M = \lambda_A/2$, such that the impurity sits at a cavity anti-node and the coupling is maximized. In analogy to conventional cavity QED, the coupling between the impurity atom and fiber should be enhanced by the number of round trips $\sim N_A\Gamma_{1D}/\Gamma'$ a photon makes within the cavity.

The spectral properties of this system are illustrated in figure 3. Here, we calculate the fields generated by an impurity atom that is driven from free space, as in figure 1(c). The driving field $\mathcal{E}$ is taken to be sufficiently weak that atomic saturation can be ignored, with the atom generating the intra-cavity field profile seen in figure 2(c). In figures 3(a) and (b), we plot the intra-cavity field intensity I_c at the impurity atom position and the intensity T_c transmitted by either atomic mirror, as a function of the drive detuning Δ_A. The observed normal mode splittings suggest that we reach the 'strong coupling' regime, where the coherent interaction strength between the impurity atom and cavity mode exceeds their individual dissipative rates [3–5, 25–27]. As shown in figure 3(c), the splitting between the two peaks $\Omega_{\pm 1}$ increases as $\Omega_{+1} - \Omega_{-1} \equiv 2g \approx \sqrt{N_A}\Gamma_{1D}$ for $N_A \lesssim N_{gap}$ and approaches a constant value in the band gap regime $N_A \gtrsim N_{gap}$. The normal mode splitting is also illustrated in figure 3(d), where we allow the resonance frequency of the impurity atom ω_I to be separately tuned from that of the mirror atoms, ω_A.

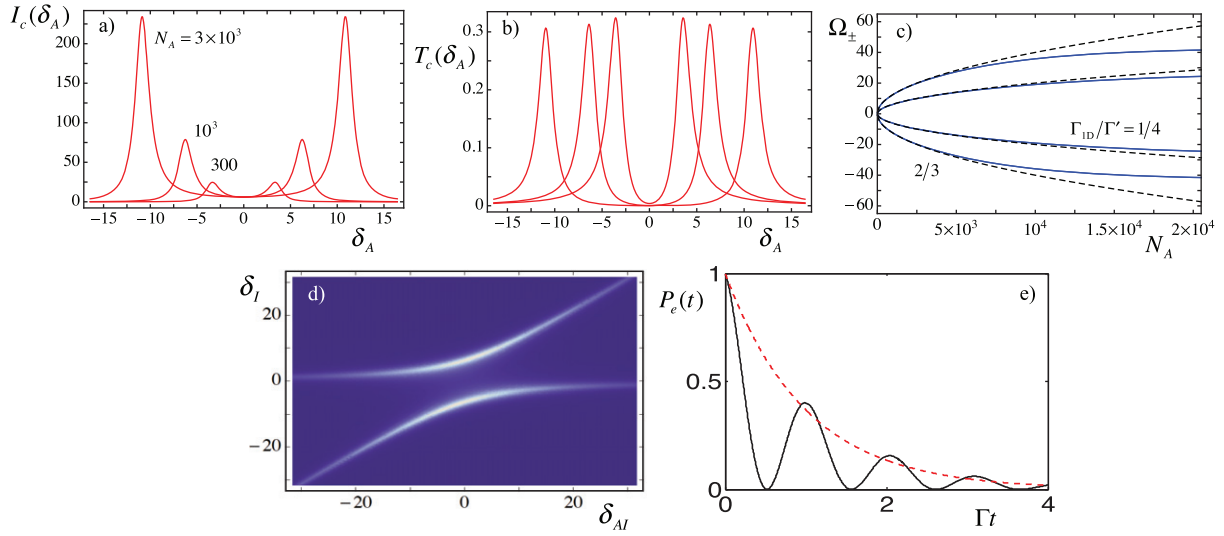## 2. From quantum spin to Jaynes–Cummings model

While these results can be derived within the transfer matrix formalism, we now present a more powerful interacting spin model that elucidates the origin of the strong coupling. The general field solution of equation (1) can be substituted into the atomic evolution equations, resulting in expressions where the evolution of atomic coherence $\dot{\sigma}_{ge}^j(t)$ for atom j depends on the coherence of other atoms k at retarded times, $\sigma_{ge}^k(t - |z_j - z_k|/v)$. Further simplification results if the atomic coherences are slowly varying, $\sigma_{ge}^j(t - \epsilon) \approx \sigma_{ge}^j(t)e^{i\omega_A\epsilon}$, and if the characteristic bandwidth $\Delta\omega$ of the dynamics satisfies $\Delta\omega L/v \ll 1$, where L is the system length. In this limit, the photon-mediated dipole–dipole interactions between atoms are described by a master equation $\dot{\rho} = -i[H_{dd}, \rho] + \mathcal{L}_{dd}[\rho]$ for the atomic density matrix ρ, where

$$H_{dd} = (\Gamma_{1D}/2) \sum_{j,k} \sin k_A|z_j - z_k| \sigma_{eg}^j \sigma_{ge}^k \tag{2}$$

and

$$\mathcal{L}_{dd}[\rho] = -(\Gamma_{1D}/2) \sum_{j,k} \cos k_A|z_j - z_k| \left(\sigma_{eg}^j \sigma_{ge}^k \rho + \rho \sigma_{eg}^j \sigma_{ge}^k - 2\sigma_{ge}^k \rho \sigma_{eg}^j \right). \tag{3}$$

Here $k_A = 2\pi/\lambda_A$ is the resonant wavevector, and the sum on j, k runs over all atoms. The Hamiltonian characterizes field-mediated dipole exchange between atoms, while the incoherent evolution $\mathcal{L}_{dd}$ characterizes cooperative emission. Interestingly, the interactions are infinite in range and sinusoidal. These features can be qualitatively understood by noting that a photon emitted by one atom into the fiber propagates without attenuation until it scatters off a second atom, and the interaction should be sensitive only to the relative phases between them. Similar equations have been previously derived within the more restrictive Born–Markov

Figure 3. Strong coupling regime of cavity QED. Figures (a–d) depict spectra for the cavity configuration of figure 1(c), with N_A total mirror atoms. (a) The impurity atom is driven by an external field $\mathcal{E}$, with dimensionless detuning $\delta_A = \Delta_A/(\Gamma/2)$ relative to all of the atoms. The intra-cavity intensity $I_c \equiv |E_R(z = 0)|^2$ exhibits a normal mode splitting with peaks at $\Omega_{\pm 1} \approx \Gamma_{1D}\sqrt{N_A}/2$. Here we have chosen $\Gamma_{1D} = \Gamma'/4$. (b) The intensity $T_c \equiv |E_R(z = z_{N_M})|^2$ transmitted by a single mirror for the same conditions as in (a). I_c and T_c are normalized to the intensity emitted by a single atom driven by the same amplitude $\mathcal{E}$ on resonance, absent the atomic mirrors. (c) Solid lines: positions of the normal mode peaks $\Omega_{\pm 1}$ for $I_c(\delta_A)$ versus atom number, for $\Gamma_{1D} = \Gamma'/4$ and $\Gamma_{1D} = 2\Gamma'/3$. The normal mode splitting is well-approximated by $\Omega_{\pm 1} = \pm\Gamma_{1D}\sqrt{N_A}/2$ (dashed lines) for atom numbers $N_A \lesssim N_{gap}$ and saturates for larger atom number. (d) Spectra for the intra-cavity intensity I_c when the detunings of the mirror atoms and impurity atom are separately tuned. Here $\delta_I = (\omega_P - \omega_I)/(\Gamma/2)$ denotes the detuning of the impurity atom relative to the probe beam, while $\delta_{AI} = (\omega_A - \omega_I)/(\Gamma/2)$ denotes the difference between the mirror and impurity atom resonance frequencies. (e) The population $P_e(t)$ of an initially excited, single impurity atom inside an atomic cavity (solid curve), which exhibits vacuum Rabi oscillations as the excitation is reversibly exchanged with a spin wave comprising the mirror atoms at a rate $g = \Gamma_{1D}\sqrt{N_A}/2$. We have used $\Gamma_{1D} = \Gamma'/4$ and $N_A = 900$ atoms. For comparison, the dashed red curve shows the spontaneous emission decay of a single excited atom absent the cavity, $P_e(t) = e^{-\Gamma t}$.

approximation [36]. Although the fields have apparently been eliminated, we note that they can be reconstructed using equation (1). We also include the effects of independent atomic emission into free space at a rate Γ' through a separate contribution $\mathcal{L}_{ind}[\rho]$ to the density matrix evolution.

Applying the spin model to the cavity QED configuration yields an interaction Hamiltonian $H_{dd} = g(\hat{s}^- \hat{S}_{cav}^+ + \text{h.c.})$, where $g \equiv \Gamma_{1D}\sqrt{N_A}/2$. Here, we have defined lowering operators $\hat{s}^- = \sigma_{ge}^{(j=0)}$ for the impurity atom and $\hat{S}_{cav}^- = N_A^{-1/2}\sum_{j>0}(\sigma_{ge}^j + \sigma_{ge}^{-j})(-1)^j$ for a cavity 'photon' consisting of a collective spin wave of the mirror atoms. $\hat{S}_{cav}^-$ is a canonical lowering operator

from which other angular momentum operators can be constructed. These operators together satisfy the usual angular momentum commutation relations, which can be used to determine the spectrum of H_{dd}.

In particular, the dipole–dipole interaction splits the nominal degeneracy between the state where n_{cav} excitations are contained in the cavity spin mode, $|g, n_{cav}\rangle \propto (\hat{S}^+_{cav})^{n_{cav}}|g\rangle^{\otimes(N_A+1)}$, and the state with $n_{cav} - 1$ excitations in the spin mode and one excitation in the impurity atom, $|e, n_{cav} - 1\rangle \propto \hat{s}^+(\hat{S}^+_{cav})^{n_{cav}-1}|g\rangle^{\otimes(N_A+1)}$. The new eigenstates are given by $|\pm, n_{cav}\rangle = (|g, n_{cav}\rangle \pm |e, n_{cav} - 1\rangle)/\sqrt{2}$, with corresponding energies $\Omega_{\pm,n_{cav}} \approx \pm g\sqrt{n_{cav}}$ in the regime of small excitation number $n_{cav} \ll N_A$ (where saturation is negligible and the mirror atom excitations are nearly bosonic). This excitation spectrum is intrinsically anharmonic and identical to that of the Jaynes–Cummings model describing a single two-level atom coupled to a conventional cavity [24]. The linear case of $n_{cav} = 1$ yields $\Omega_{\pm,1} = \pm\Gamma_{1D}\sqrt{N_A}/2$, reproducing the splitting in the spectrum observed in figure 3 for $N_M \lesssim N_{gap}$. This mapping onto the Jaynes–Cummings model is important in two respects. Firstly, its nonlinearity is known to be critical to various tasks in quantum information processing based on cavity QED [2]. Secondly, the ability to reduce our *a priori* multi-mode atomic ensemble to a single mode enables relatively simple dynamics and exact solutions, which are generally absent in the multi-mode case [37]. This feature enables tasks in quantum information to be executed with reduced errors and high fidelity.

The dissipation rates of the cavity configuration can be similarly characterized, by writing $\mathcal{L}_{dd}[\rho] = -(\Gamma_{1D}/2)(\hat{s}^+\hat{s}^-\rho + \rho\hat{s}^+\hat{s}^- - 2\hat{s}^-\rho\hat{s}^+) - (N_A\Gamma_{1D}/2)(\hat{S}^+_{rad}\hat{S}^-_{rad}\rho + \rho\hat{S}^+_{rad}\hat{S}^-_{rad} - 2\hat{S}^-_{rad}\rho\hat{S}^+_{rad})$. Here $\hat{S}^-_{rad} = N_A^{-1/2}\sum_{j>0}(\sigma^j_{ge} - \sigma^{-j}_{ge})(-1)^{j+1}$ is a lowering operator for a spin wave of the mirror atoms with super-radiant emission. While angular momentum operators constructed from $\hat{S}^-_{rad}$ obey canonical commutation relations among themselves, the two spin waves associated with $\hat{S}^-_{cav}$ and $\hat{S}^-_{rad}$ have non-trivial commutation relations between them. For example, $\hat{S}^-_{rad}|1_{cav}\rangle = 0$, indicating that a single cavity excitation does not emit into the waveguide. Thus, its decay rate is given by the single-atom emission rate into free space, $\kappa = \Gamma'$. The origin of the sub-radiance is destructive interference between the light emitted by pairs of mirror atoms on each side of the impurity (say $\pm j$), as illustrated in figure 1(c). Here, one sees that each atom in the pair $\pm j$ has the same phase $(-1)^j$. However, because they are spaced an odd multiple of $\lambda_A/2$ apart, their radiation fields into the waveguide perfectly cancel. This effect also gives rise to the high transmitted intensity T_c of light produced by the impurity atom (figure 3(b)). Interestingly, applying $\mathcal{L}_{dd}$ to the spin wave of only a single mirror (say $1 \leqslant j \leqslant N_M$) reveals that such a state is maximally super-radiant, giving rise to its high reflectance. Likewise, one can show that the decay rate of the state $|e, 0_{cav}\rangle$ (an excited impurity atom) is $\Gamma = \Gamma_{1D} + \Gamma'$.

In analogy with cavity QED, one can associate various figures of merit to g, κ, Γ. For example, the enhanced coupling to the cavity mode by the impurity atom is characterized by the cooperativity $C \equiv \frac{g^2}{\kappa\Gamma} = \frac{\Gamma_{1D}}{\Gamma_{1D}+\Gamma'}\frac{N_A\Gamma_{1D}}{\Gamma'}$. Note that $\frac{\Gamma_{1D}}{\Gamma_{1D}+\Gamma'}$ represents the single-atom coupling efficiency to the waveguide, while $\frac{N_A\Gamma_{1D}}{\Gamma'}$ is proportional to the cavity finesse (figure 2(b)). Surprisingly, our results also show that with modest atom numbers one can reach the strong coupling regime $g > \kappa, \Gamma$, where an impurity atom can emit and then reabsorb the same photon (the so-called vacuum Rabi oscillations [24, 25]).

In contrast to the transfer matrix formalism, our interacting spin model is ideal for studying the system dynamics in the quantum regime. In figure 3(e), we plot the analytic solution for the time evolution $\dot{\rho}$ starting with an initially excited impurity atom ($\rho = |e, 0_{cav}\rangle\langle e, 0_{cav}|$ at
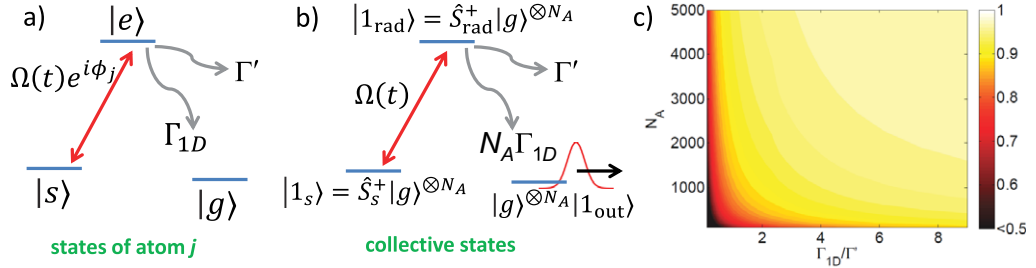
$t = 0$). Rabi oscillations of the impurity excited state population are clearly visible in the case of $N_A = 900$ atoms and $\Gamma_{1D} = \Gamma'/4$ ($g = 3\Gamma$, $\kappa = 0.8\Gamma$). This feature can be viewed in the dressed-state picture as an interference effect between the states $|\pm, 1_{cav}\rangle$ which make up the initial state.

The strong coupling regime for a single impurity atom can be reached with very low finesse for the atomic mirrors (e.g. $F \sim 590$ in figure 3(a) with $N_A = 3000$ atoms, while $F \sim 175$ in figure 3(e) with $N_A = 900$ atoms; see figure 2(b)). By contrast, for a conventional Fabry–Perot cavity with dielectric mirrors, strong coupling requires finesse $F \gtrsim 10^5$ [3]. In fact, the decay rate κ relevant to strong coupling with atomic mirrors as in figure 1(c) is that of the sub-radiant mode of the atomic chain ($\kappa = \Gamma'$). The highly dispersive nature of these atoms causes κ to be much smaller than the conventional cavity decay rate $\kappa_c = v\pi/F L_{eff}$, where L_{eff} is the effective cavity length and F is the finesse set by the mirror reflectivity. In this regard, note that the sub-radiant mode is not relevant to the dielectric coating of a conventional high-reflectivity mirror because of the rapid relaxation of the polarizability of the dielectric elements. Furthermore, although we have focused on the case of perfect filling of the atomic mirror lattice sites, it is clear from the infinite-range, sinusoidal form of the interactions that these effects are quite robust to filling imperfections and rely solely on the system periodicity.

3. Building blocks for scalable quantum information processing

Here, we describe how our cavity QED system can be used to realize the basic building blocks for scalable quantum information processing. As with other atom–light interfaces [1, 2], the utility of the present system is greatly extended by introducing an atomic meta-stable state $|s\rangle$ (see figure 4(a)), which is decoupled from the fiber modes due to an orthogonal dipole orientation, but which can be coupled to $|e\rangle$ through a time-dependent external optical field with strength $\Omega(t)e^{i\phi_j}$ for atom j. Here we assume that the Rabi amplitude $\Omega(t)$ is identical for all atoms, but we allow for the possibility of a varying phase ϕ_j, which can be used to couple to selective spin waves. As we now describe, this coupling can be used to faithfully map the quantum states of propagating waveguide photons into meta-stable spin wave excitations and back to provide a long-lived quantum memory. The coupling also enables these meta-stable spin wave excitations to be loaded into the cavity, which allows for quantum logic and other non-classical operations to be performed.

We first investigate the mapping of a single, meta-stable spin wave excitation in the atom mirrors to an outgoing photon. The spin wave of interest is characterized by the operator $\hat{S}_s^- = N_A^{-1/2} \sum_{j>0} (\sigma_{gs}^j - \sigma_{gs}^{-j})(-1)^{j+1}$, such that the initial state of the mirror atoms is given by $|1_s\rangle \equiv \hat{S}_s^+|g\rangle^{\otimes N_A}$. The impurity atom is assumed to be in state $|s\rangle$ and undriven by external fields, so that it does not participate in this process. The external field $\Omega(t)e^{i\phi_j}$ driving the mirror atoms couples $|1_s\rangle$ to the super-radiant, excited-state spin wave $|1_{rad}\rangle \equiv \hat{S}_{rad}^+|g\rangle^{\otimes N_A}$ if the driving phase for the atoms is equal, say $\phi_j = 0$, as shown in figure 4(b). Note that $|1_{rad}\rangle$ couples with maximum spontaneous emission rate $N_A\Gamma_{1D}$ into the waveguide, compared to Γ' into free space. This feature of $|1_{rad}\rangle$ enables efficient mapping of the meta-stable spin wave $|1_s\rangle$ into an outgoing photon $|1_{out}\rangle$ in the waveguide. Generally, a proper choice of $\Omega(t)$ can produce an outgoing photon of any desired shape within a bandwidth $\lesssim N_A\Gamma_{1D}$, and with an error probability of $\Gamma'/N_A\Gamma_{1D}$ due to free-space leakage [28, 38, 39]. It should be noted that the outgoing photon is split equally into left- and right-propagating modes, due to the symmetry of the super-radiant spin wave. This photon split between counter-propagating modes

Figure 4. Building blocks for quantum information processing. (a) Three-level structure of a single atom. The ground state $|g\rangle$ is coupled via waveguide modes to excited state $|e\rangle$, while a meta-stable state $|s\rangle$ is decoupled from the waveguide but can be coupled to $|e\rangle$ through an external control field $\Omega(t)e^{i\phi_j}$. The excited state decays into free space and the waveguide at rates Γ', Γ_{1D}, respectively. (b) The collective states of the cavity mirror atoms used to efficiently map between atomic excitations and propagating photons. With a proper choice of driving phases ϕ_j, the external field $\Omega(t)$ couples a meta-stable spin excitation $|1_s\rangle$ in the mirror atoms to a super-radiant, excited-state spin wave $|1_{\rm rad}\rangle$. This state emits into the waveguide at an enhanced rate $N_A\Gamma_{1D}$, generating an outgoing photon $|1_{\rm out}\rangle$ with high probability. The time-reversed process enables an incoming photon to be converted to a meta-stable spin excitation. (c) Fidelity for quantum state transfer between two impurities p, q in a cavity formed by N_A mirror atoms exterior to the impurities (see figure 1(d)). The fidelity of the adiabatic transfer process is numerically optimized as functions of the single-atom coupling strength to the waveguide (Γ_{1D}/Γ') and mirror atom number N_A.

can subsequently be recombined into a single output port of an external beam splitter, provided that this interferometric setup is properly phase-stabilized.

By time reversal symmetry [38–40], it also follows that an incoming photon in the waveguide (in an equal superposition of left- and right-propagating modes) of bandwidth $\lesssim N_A\Gamma_{1D}$ can be mapped into a spin excitation $|1_s\rangle$ starting from an initial atomic mirror state $|g\rangle^{\otimes N_A}$ with the same error $\Gamma'/N_A\Gamma_{1D}$. These mappings to and from $|1_s\rangle$ thus provide an efficient interface between propagating fields and the atomic ensemble.

In addition, $|1_s\rangle$ can be efficiently coupled to a cavity excitation $|1_{\rm cav}\rangle \equiv \hat{S}^+_{\rm cav}|g\rangle^{\otimes N_A}$ by choosing a different relative phase for the control field, e.g. $\phi_j = 0$ for $j > 0$ and $\phi_j = \pi$ for $j < 0$. These separate processes of mapping $|1_s\rangle$ between outgoing photons and cavity excitations are necessary in our system because the cavity excitation is nominally decoupled from the waveguide (being maximally sub-radiant). From here, however, our system behaves identically to a conventional cavity QED system governed by the Jaynes–Cummings model. In particular, one can apply to our system existing information processing protocols such as for conditional quantum logic between two photons [41] or impurity atoms [42], or quantum state transfer between two such atoms [42].

As a specific example, we analyze how our system can serve as an efficient quantum information bus between two distant impurity atoms within the same chain, in analogy to the case of two atoms in a conventional cavity [42]. One possible configuration is illustrated in figure 1(d), where two well-separated impurity atoms p, q are initially embedded in a long

chain of mirror atoms in state $|g\rangle$. To facilitate information transfer, the mirror atoms between p, q are first flipped into the transparent meta-stable state $|s\rangle$, and thus do not participate in the process. Through this operation, the impurity atoms are loaded into a new, common cavity mode, which is defined by the mirror atoms external to p, q and which mediates coherent information transfer between the two impurities. The objective of the state transfer process is to map an arbitrary quantum bit encoded in the states s, g from p to q, i.e. $(c_1|s_p\rangle + c_2|g_p\rangle)|g_q\rangle \to |g_p\rangle(c_1|s_q\rangle + c_2|g_q\rangle)$. We assume that the impurity atoms can be driven by individual external control fields $\Omega_{p,q}(t)$ on the $|s\rangle - |e\rangle$ transition. These control beams clearly have no effect on the state $|g_p, g_q\rangle$, and we describe how a proper choice of the control fields yields $|s_p, g_q\rangle \to |g_p, s_q\rangle$ to enable the desired transfer of an arbitrary superposition. As noted in [42], there exists an instantaneous dark eigenstate of the system Hamiltonian given by $|D(t)\rangle \propto g\Omega_q(t)|s_p, g_q, 0_{\rm cav}\rangle + g\Omega_p(t)|g_p, s_q, 0_{\rm cav}\rangle - \Omega_p(t)\Omega_q(t)|g_p, g_q, 1_{\rm cav}\rangle$. Note that the state $|s_p, g_q\rangle$ ($|g_p, s_q\rangle$) corresponds to $|D(t)\rangle$ in the limit where $\Omega_p = 0$ ($\Omega_q = 0$). The desired transformation can thus be achieved through adiabatic passage using a pulse sequence that leads from $\Omega_p(t = 0) = 0$ to $\Omega_q(T) = 0$ over a time $T \gg 1/g, 1/\Omega_0$, where Ω_0 is the characteristic amplitude of $\Omega_{p,q}$. Since $|D(t)\rangle$ and $|g_p, g_q\rangle$ have the same energy, coherence of an arbitrary superposition is maintained throughout the process.

In figure 4(c), we plot the fidelity of the transformation $|s_p, g_q\rangle \to |g_p, s_q\rangle$ as functions of $\Gamma_{\rm 1D}/\Gamma'$ and mirror atom number $N_{\rm A}$ (determined by the number of atoms external to p, q). Note that this represents the lower bound on the transfer fidelity of an arbitrary state, as the state $|g_p, g_q\rangle$ is unaffected by the pulse sequence. Here we have chosen the pulse sequence $\Omega_p(t) = \Omega_0 \sin\frac{\pi t}{2T}$ and $\Omega_q(t) = \Omega_0 \cos\frac{\pi t}{2T}$ ($0 \leqslant t \leqslant T$) with overall pulse duration $T = 50/g$, and we have optimized Ω_0 by numerically solving our spin model. The optimized error of the state transfer process depends on the cavity cooperativity factor approximately as $\sim 1/\sqrt{C}$, which reflects an optimized balance between dissipation of the cavity excitation component of the dark state $|D\rangle$ and non-adiabatic transitions out of the dark state. A unique feature of our system compared to a conventional cavity is that the coupling strength g does not decrease with increasing cavity mode volume (i.e. increasing separation between p, q), so that the amount of time required for the adiabatic process remains constant.

4. Possible implementations and outlook

One of the attractive features of our proposed route to single-atom, single-photon strong coupling is that it can be attained with parameters that are already within reach of present capabilities. Recent experiments have demonstrated the trapping of $N_{\rm A} \sim 10^3$ atoms near a tapered nanofiber with single-atom coupling efficiencies of $\Gamma_{\rm 1D}/\Gamma' \sim 0.1$ [15]. The coupling between atoms and the evanescent fields of the guided modes can be further increased to values of $\Gamma_{\rm 1D}/\Gamma' \sim 0.2$ by trapping closer to the nanofiber surface and to $\Gamma_{\rm 1D}/\Gamma' \sim 1$ by using higher-index waveguiding materials [43]. An interesting alternative would be to couple trapped atoms to photonic crystal nanowires [44], where values of $\Gamma_{\rm 1D}/\Gamma' > 1$ should be achievable by tailoring the photonic band structure around the resonance frequency of the atoms. This tailoring of the dispersion relation could further be used to provide commensurate wavevectors between the trapping and resonant light. We thus anticipate that cooperativities of $C \sim 10$ are possible with present systems while simultaneously reaching the strong coupling regime $g > \kappa, \Gamma$, and that an order-of-magnitude improvement in the cooperativity is possible in the near future.

IOP Institute of Physics Φ DEUTSCHE PHYSIKALISCHE GESELLSCHAFT

A key challenge to realizing the quantum information protocols described above is the need to specially designate one or more atoms to be 'impurities' that are trapped with a different lattice spacing than the mirror atoms. One possible implementation could be to create atomic traps with relatively large lattice constants (e.g. several integer multiples of $\lambda_A/2$), which would enable selective manipulation of individual atoms within the lattice. Alternatively, non-uniform structure, such as adiabatic changes in the fiber diameter, could allow for the necessary differences in propagation phases between the location of the impurity atom and other sites. This could be naturally implemented in photonic crystal nanowires, where local fine-tuning of the periodic holes that form the band structure is often used to introduce localized states [44].

In summary, we have described a novel technique to realize and manipulate strong photon-atom coupling using cold atoms trapped near a tapered nanofiber [13–15]. Our approach combines concepts from cavity QED, collective enhancement in atomic ensembles, and tight focusing of optical fields to achieve the strong coupling regime using relatively modest resources, and can be used for scalable quantum information processing.

Thus far, we have investigated the case of a single excitation, but we anticipate that nonlinear and many-body behavior involving atoms and photons [45–47] will be an interesting topic for further exploration. For example, this system may allow for the experimental study of quantum spin models with infinite-range interactions [48]. This system could also stimulate interesting studies into the role of atomic disorder in field propagation [49] and its interplay with interactions [50]. Furthermore, the ability to map cavity excitations onto long-lived atomic quantum memories and subsequently to output fields can enable the generation of non-classical, many-photon states (e.g. using the techniques of [51]), which find applications in areas such as enhanced quantum metrology and sensing [52]. We also anticipate that a rich set of phenomena can be explored if trapped atoms can be coupled to photonic crystal nanowires. More exotic interactions between atoms could occur by introducing broken translational invariance into these nanowires. Moreover, these structures could contain additional degrees of freedom, such as mechanical modes [44], to which atoms can provide a quantum interface [20].

Acknowledgments

References

[1] Duan L-M and Monroe C 2008 Robust probabilistic quantum information processing with atoms, photons and atomic ensembles *Adv. At. Mol. Opt. Phys.* **55** 419–63
[2] Kimble H J 2008 The quantum internet *Nature* **453** 1023–30
[3] Miller R, Northup T E, Birnbaum M, Boca A, Boozer A D and Kimble H J 2005 Trapped atoms in cavity QED: coupling quantized light and matter *J. Phys. B: At. Mol. Opt. Phys.* **38** S551–65

IOP Institute of Physics ◉ DEUTSCHE PHYSIKALISCHE GESELLSCHAFT

[4] Walther H, Varcoe B T H, Englert B-G and Becker T 2006 Cavity quantum electrodynamics *Rep. Prog. Phys.* **69** 1325–82

[5] Haroche S and Raimond J M 2006 *Exploring the Quantum: Atoms, Cavities and Photons* (New York: Oxford University Press)

[6] Hammerer K, Sørensen A S and Polzik E S 2010 Quantum interface between light and atomic ensembles *Rev. Mod. Phys.* **82** 1041–93

[7] van Enk S J and Kimble H J 2001 Strongly focused light beams interacting with single atoms in free space *Phys. Rev.* A **63** 023809

[8] Darquié B, Jones M P A, Dingjan J, Beugnon J, Bergamini S, Sortais Y, Messin G, Browaeys A and Grangier P 2005 Controlled single-photon emission from a single trapped two-level atom *Science* **309** 454–6

[9] Wrigge G, Gerhardt I, Hwang J, Zumofen G and Sandoghdar V 2008 Efficient coupling of photons to a single molecule and the observation of its resonance fluorescence *Nature Phys.* **4** 60–6

[10] Akimov A V, Mukherjee A, Yu C L, Chang D E, Zibrov A S, Hemmer P R, Park H and Lukin M D 2007 Generation of single optical plasmons in metallic nanowires coupled to quantum dots *Nature* **450** 402–6

[11] Tey M K, Chen Z, Aljunid S A, Chng B, Huber F, Maslennikov G and Kurtsiefer C 2008 Strong interaction between light and a single trapped atom without the need for a cavity *Nature Phys.* **4** 924–7

[12] Hétet G, Slodička Hennrich M and Blatt R 2011 Single atom as a mirror of an optical cavity *Phys. Rev. Lett.* **107** 133002

[13] Nayak K P, Melentiev P N, Morinaga M, Le Kien F, Balykin V I and Hakuta K 2007 Optical nanofiber as an efficient tool for manipulating and probing atomic fluorescence *Opt. Express* **15** 5431–8

[14] Vetsch E, Reitz D, Sagué G, Schmidt R, Dawkins S T and Rauschenbeutel A 2010 Optical interface created by laser-cooled atoms trapped in the evanescent field surrounding an optical nanofiber *Phys. Rev. Lett.* **104** 203603

[15] Goban A, Choi K S, Alton D J, Ding D, Lacroûte C, Pototschnig M, Thiele T, Stern N P and Kimble H J 2012 Demonstration of a state-insensitive, compensated nanofiber trap arXiv:1203.5108

[16] Lacroûte C, Choi K S, Goban A, Alton D J, Ding D, Stern N P and Kimble H J 2012 A state-insensitive, compensated nanofiber trap *New. J. Phys.* **14** 023056

[17] Colombe Y, Steinmetz T, Dubois G, Linke F, Hunger D and Reichel J 2007 Strong atom-field coupling for Bose–Einstein condensates in an optical cavity on a chip *Nature* **450** 272–6

[18] Alton D J, Stern N P, Aoki T, Lee H, Ostby E, Vahala K J and Kimble H J 2011 Strong interactions of single atoms and photons near a dielectric boundary *Nature Phys.* **7** 159–65

[19] Treutlein P, Hunger D, Camerer S, Hänsch T W and Reichel J 2007 Bose–Einstein condensate coupled to a nanomechanical resonator on an atom chip *Phys. Rev. Lett.* **99** 140403

[20] Hammerer K, Wallquist M, Genes C, Ludwig M, Marquardt F, Treutlein P, Zoller P, Ye J and Kimble H J 2009 Strong coupling of a mechanical oscillator and a single atom *Phys. Rev. Lett.* **103** 063005

[21] Renn M J, Montgomery D, Vdovin O, Anderson D Z, Wieman C E and Cornell E A 1995 Laser-guided atoms in hollow-core optical fibers *Phys. Rev. Lett.* **75** 3253–6

[22] Londero P, Venkataraman V, Bhagwat A R, Slepkov A D and Gaeta A L 2009 Ultralow-power four-wave mixing with rb in a hollow-core photonic band-gap fiber *Phys. Rev. Lett.* **103** 043602

[23] Bajcsy M, Hofferberth S, Balic V, Peyronel T, Hafezi M, Zibrov A S, Vuletic V and Lukin M D 2009 Efficient all-optical switching using slow light within a hollow fiber *Phys. Rev. Lett.* **102** 203902

[24] Jaynes E T and Cummings F W 1963 Comparison of quantum and semiclassical radiation theories with application to the beam maser *Proc. IEEE* **51** 89–109

[25] Sanchez-Mondragon J J, Narozhny N B and Eberly J H 1983 Theory of spontaneous-emission line shape in an ideal cavity *Phys. Rev. Lett.* **51** 550–3

[26] Thompson R J, Rempe G and Kimble H J 1992 Observation of normal-mode splitting for an atom in an optical cavity *Phys. Rev. Lett.* **68** 1132–5

[27] Brune M, Schmidt-Kaler F, Maali A, Dreyer J, Hagley E, Raimond J M and Haroche S 1996 Quantum rabi oscillation: a direct test of field quantization in a cavity *Phys. Rev. Lett.* **76** 1800–3

[28] Chang D E, Sørensen A S, Demler E A and Lukin M D 2007 A single-photon transistor using nanoscale surface plasmons *Nature Phys.* **3** 807–12

[29] Deutsch I H, Spreeuw R J C, Rolston S L and Phillips W D 1995 Photonic band gaps in optical lattices *Phys. Rev.* A **52** 1394–410

[30] Chang Y, Gong Z R and Sun C P 2011 Multiatomic mirror for perfect reflection of single photons in a wide band of frequency *Phys. Rev.* A **83** 013825

[31] Birkl G, Gatzke M, Deutsch I H, Rolston S L and Phillips W D 1995 Bragg scattering from atoms in optical lattices *Phys. Rev. Lett.* **75** 2823–6

[32] Schilke A, Zimmermann C, Courteille P W and Guerin W 2011 Photonic band gaps in one-dimensionally ordered cold atomic vapors *Phys. Rev. Lett.* **106** 223903

[33] Petrosyan D 2007 Tunable photonic band gaps with coherently driven atoms in optical lattices *Phys. Rev.* A **76** 053823

[34] Zoubi H and Ritsch H 2010 Hybrid quantum system of a nanofiber mode coupled to two chains of optically trapped atoms *New J. Phys.* **12** 103014

[35] Shen J T and Fan S 2005 Coherent photon transport from spontaneous emission in one-dimensional waveguides *Opt. Lett.* **30** 2001–3

[36] Le Kien F, Dutta Gupta S, Nayak K P and Hakuta K 2005 Nanofiber-mediated radiative transfer between two distant atoms *Phys. Rev.* A **72** 063815

[37] Hafezi M, Chang D E, Gritsev V, Demler E A and Lukin M D 2011 Photonic quantum transport in a nonlinear optical fiber *Europhys. Lett.* **94** 54006

[38] Gorshkov A V, André A, Fleischhauer M, Sorensen A S and Lukin M D 2007 Universal approach to optimal photon storage in atomic media *Phys. Rev. Lett.* **98** 123601

[39] Gorshkov A V, André A, Lukin M D and Sørensen A S 2007 Photon storage in Λ-type optically dense atomic media II. Free-space model *Phys. Rev.* A **76** 033805

[40] Cirac J I, Zoller P, Kimble H J and Mabuchi H 1997 Quantum state transfer and entanglement distribution among distant nodes in a quantum network *Phys. Rev. Lett.* **78** 3221–4

[41] Duan L-M and Kimble H J 2004 Scalable photonic quantum computation through cavity-assisted interactions *Phys. Rev. Lett.* **92** 127902

[42] Pellizzari T, Gardiner S A, Cirac J I and Zoller P 1995 Decoherence, continuous observation and quantum computing: a cavity QED model *Phys. Rev. Lett.* **75** 3788–91

[43] Klimov V V and Ducloy M 2004 Spontaneous emission rate of an excited atom placed near a nanofiber *Phys. Rev.* A **69** 013812

[44] Eichenfield M, Chan J, Camacho R M, Vahala K J and Painter O 2009 Optomechanical crystals *Nature* **462** 78–82

[45] Gorshkov A V, Otterbach J, Demler E, Fleischhauer M and Lukin M D 2010 Photonic phase gate via an exchange of Fermionic spin waves in a spin chain *Phys. Rev. Lett.* **105** 060502

[46] Kiffner M and Hartmann M J 2010 Dissipation-induced Tonks–Girardeau gas of polaritons *Phys. Rev.* A **81** 021806

[47] Shahmoon E, Kurizki G, Fleischhauer M and Petrosyan D 2011 Strongly interacting photons in hollow-core waveguides *Phys. Rev.* A **83** 033806

[48] Lipkin H J, Meshkov N and Glick A J 1965 Validity of many-body approximation methods for a solvable model: (I). Exact solutions and perturbation theory *Nucl. Phys.* **62** 188–98

[49] Kirkman P D and Pendry J B 1984 The statistics of one-dimensional resistances *J. Phys. C: Solid State Phys.* **17** 4327

[50] Giamarchi T and Schulz H J 1988 Anderson localization and interactions in one-dimensional metals *Phys. Rev.* B **37** 325–40

[51] Law C K and Eberly J H 1996 Arbitrary control of a quantum electromagnetic field *Phys. Rev. Lett.* **76** 1055–8

[52] Dowling J P 2008 Quantum optical metrology—the lowdown on high-N00N states *Contemp. Phys.* **49** 125–43